

Case study

Some observations on the wear of diamond tools in ultra-precision cutting of single-crystal silicon[☆]

Jiwan Yan^{a,*}, Katsuo Syoji^b, Jun'ichi Tamaki^a

^a Department of Mechanical Engineering, Kitami Institute of Technology, Koen-cho 165, Kitami, Hokkaido 090-8507, Japan

^b Department of Mechatronics and Precision Engineering, Tohoku University, Aramaki-Aoba-01, Aoba-ku, Sendai 980-8579, Japan

Abstract

Single-crystal silicon is not only a dominant substrate material for the fabrication of micro-electro and micro-mechanical components but also an important infrared optical material. Since silicon is a nominally brittle material, currently it is finished by grinding, lapping and chemo-mechanical polishing (CMP). However, silicon can be deformed plastically in machining, yielding ductile chips under the influence of high hydrostatic pressure. Therefore, an alternate approach would be to machine silicon with a single point tool in the ductile mode without the need for subsequent polishing. This way damage due to brittle fracture can be minimized and the productivity of complex-shaped components can be significantly improved. This technology involves the use of an extremely rigid, ultra-precision machine tool and a single-crystal diamond tool with a high negative rake angle. However, one of the problems existing in the industrial application of the ductile machining technology is the wear of diamond tools. Tool wear not only raises the machining cost but also degrades the product quality. The tool wear problem becomes particularly serious when machining large radius components. This paper deals with the performance of diamond cutting tools during single point diamond turning of single-crystal silicon substrates at a machining scale smaller than 1 μm . The cutting edge, the finished surface and the cutting chips were examined by scanning electron microscope (SEM) and the micro-cutting forces were measured. It was found that the tool wear could be generally classified into two types: micro-chippings and gradual wear, the predominant wear mechanism depending on undeformed chip thickness. In ductile mode cutting, flank wear was predominant and the flank wear land was characterized by trailing micro-grooves and step structures. The tool wear causes micro-fracturing on machined surface, yields discontinuous chips and raises cutting forces and force ratio. Experimental results also indicate that it is possible to prolong the ductile cutting distance by using an appropriate coolant.

© 2003 Elsevier Science B.V. All rights reserved.

Keywords: Single-crystal silicon; Ultra-precision cutting; Diamond turning; Ductile regime machining; Tool wear

1. Introduction

Single-crystal silicon is not only a dominant substrate material for the fabrication of micro-electro and micro-mechanical components but also an important infrared optical material. Since silicon is a nominally hard and brittle material, it is currently finished by lapping and chemo-mechanical polishing (CMP). However, silicon can be deformed plastically in ultra-precision cutting, yielding ductile chips and smooth surfaces [1–6]. This requires the use of an extremely rigid, environmentally controlled ultra-precision machine tool and a single-crystal diamond cutting tool with a negative rake angle. Also, the machin-

ing scale (undeformed chip thickness) must be controlled to be extremely small, down to the range of a few tens of nanometres, so that a high hydrostatic pressure will be yielded in the cutting region [5,6]. This approach can machine silicon in a ductile mode without the need for subsequent polishing. This way the productivity of aspherical and diffractive optical components and large-scale semiconductor substrates for micro-electronic mechanical system (MEMS) applications can be significantly improved [7].

However, in practice ductile regime machining of silicon is often limited by rapid wear of diamond tools. Although a diamond tool can be used to cut nonferrous metals such as aluminium and copper for a distance up to a few hundreds of kilometres [8], when cutting silicon an initially sharp tool will wear and become worn out rapidly. As the geometry of the contact zone between the tool tip and the workpiece is extremely important for the attainment of plastic flow rather than fracture in cutting, the wear of the diamond tool becomes a limiting factor in developing machining process for

[☆] This paper was unable to be presented by the author at the 14th International Conference on Wear of Materials due to the prevailing political situation at the time.

* Corresponding author. Tel.: +81-157-26-9206; fax: +81-157-23-9375. E-mail address: yanjw@mail.kitami-it.ac.jp (J. Yan).

silicon. Tool wear not only raises machining cost but also degrades product quality. This problem becomes particularly serious when machining large components [9]. For this reason, a better understanding of the performance of diamond tools in silicon machining will result in significant production cost savings. Various workers in the past have made contributions to the understanding of the processes that take place when a diamond tool wears [10–15]. However, most of the work carried out has involved the wear of diamond tools in cutting metal materials. Up to date, there is little available literature on the tool wear in silicon machining.

This paper describes some experimental results on the wear of diamond tools in single point diamond turning tests of single-crystal silicon. As a complete understanding of the wear of diamond tools can only follow understanding of the individual mechanism, this paper is focused exclusively on the effect of undeformed chip thickness on tool wear. The results involve the scanning electron microscope (SEM) observation of cutting edges, finished surface and cutting chips, as well as the measurement of surface roughness and micro-cutting forces.

2. Experimental

2.1. Experimental set up

The experiments were carried out on a TOYODA 20-25N ultra-precision lathe, the schematic of which is shown in Fig. 1. The machine has a hydrostatic bearing spindle and two perpendicular slide tables along *x*- and *z*-axis, respectively. The slide table driving system has a two-level structure: a hydraulic system for coarse motion and a servomotor system for fine motion. A precision tool post is installed on the *z*-axis table. This tool post can rotate along the vertical *B*-axis and enables the adjustment of cutting edge angle with a resolution better than 0.01°. Four air mounts were set under the machine base to isolate the environmental vibration. To measure micro-cutting forces, a special tool holder

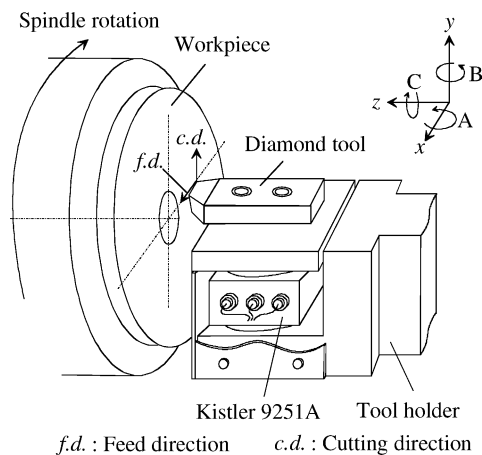


Fig. 1. Schematic of the experimental set up.

equipped with a three-component piezoelectric dynamometer (Kistler 9251A) was fabricated.

2.2. Specimens

Single-crystal silicon (111) wafers were used as specimens. These wafers are 76.2 mm in diameter, 1.2 mm in thickness and obtained with lapped finishes. To avoid cutting the workpiece centre where the cutting speed approaches zero, the centre area of the wafer within a diameter of 20 mm has been removed before experiment. Wafers were bonded on diamond turned aluminium blanks using a heat-soften glue and then vacuum chucked on the machine spindle. For the purpose of removing the lap-damaged layer, facing cuts were performed with other diamond tools different from those used for experiments, providing a mirror-like surface.

2.3. Diamond tools

Most of previous studies on diamond turning of brittle materials involve the use of a round-nosed diamond tool [1–4,9,13,16]. In this case both undeformed chip thickness and edge orientation will change as the position of cutting point changes along the round cutting edge, leading to difficulties in identifying their individual effects on tool wear.

Instead of the round-nosed tool, Yan et al. [6] proposed a straight-nosed diamond tool for ductile regime turning. In this case, as schematically shown in Fig. 2, both of the undeformed chip thickness and the edge orientation are uniform across the entire width of the cutting edge. Undeformed chip thickness *h* is independent of depth of cut *a*, and is determined by tool feed *f* and cutting edge angle κ , according to equation

$$h = f \sin \kappa. \tag{1}$$

Therefore, through the use of a sufficiently small cutting edge angle κ or a sufficiently small tool feed *f*, the proposed method makes it possible to thin the undeformed chip thickness to the nanometric range over the entire cutting region. This tool geometry also provides significant width to undeformed chip thickness ratio to ensure plane strain conditions hence the relationships among the cutting behaviour, the tool wear pattern and the undeformed chip thickness are unambiguous and readily studied.

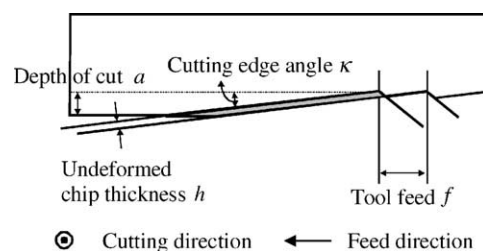


Fig. 2. Schematic of the cutting model of a straight-nosed diamond tool [6].

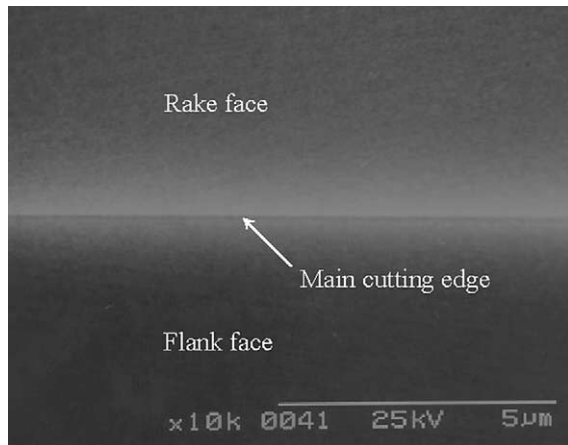


Fig. 3. SEM photograph of the main cutting edge of an unused single-crystal diamond tool.

In the experiments of the present paper, cutting tests were carried out using four straight-nosed diamond tools which have the same geometry and crystal orientation. These tools have 1.2–1.5 mm main cutting edges, 135° included angles, 0° nominal rake angles and 6° relief angles. The rake faces of these tools are in accordance with the $\{110\}$ planes and the main cutting edges are in accordance with the $\langle 100 \rangle$ directions. Before cutting, all these tools were examined using an SEM and the edge radius of these tools were estimated to be within the range of 20–50 nm. Fig. 3 is an SEM photograph of the main cutting edge of an unused diamond tool. The edge appears to be extremely smooth and sharp without any visible defects. In all the experiments, the actual tool rake angle were adjusted to -20° with steel spacers in order to achieve both high hydrostatic pressure conditions and relatively lower cutting forces [17].

2.4. Cutting conditions

The experimental conditions are listed in Table 1. Undeformed chip thickness h was set to 90 and 900 nm by adjusting cutting edge angle κ to 0.52 and 5.16° , respectively,

Table 1
Cutting conditions

Diamond tool	Single-crystal diamond straight-nosed tool
Crystal orientation	Rake face: $\{110\}$, main cutting edge: $\langle 100 \rangle$
Rake angle ($^\circ$)	-20 (nominal: 0)
Relief angle ($^\circ$)	26 (nominal: 6)
Work-material	Single-crystal silicon (111)
Depth of cut (μm)	1 and 2
Feed rate ($\mu\text{m}/\text{rev}$)	10
Undeformed chip thickness (nm)	60, 90 and 900
Cutting speed (m/min)	94–358
Cutting environment	Dry, kerosene mist, water

and keeping tool feed f constant to $10 \mu\text{m}$. As known from the previous experimental results [6], the undeformed chip thickness of 90 nm is just below the minimum critical chip thickness (or critical depth, $d_c = 92 \text{ nm}$) for ductile–brittle transition thus it corresponds to the largest material removal rate in ductile regime; whereas the undeformed chip thickness of 900 nm corresponds to a completely brittle mode cutting. Depth of cut a was set to $1 \mu\text{m}$ for $h = 90 \text{ nm}$ and $2 \mu\text{m}$ for $h = 900 \text{ nm}$, respectively. The rotation rate of machine spindle was set to 1500 rpm, consequently the cutting speed changes from 94 to 358 m/min during a facing cut. Dry cutting was first performed for the purpose of collecting chips for observation. Subsequently, kerosene mist and water were used as coolants in order to investigate the effect of coolant on tool wear.

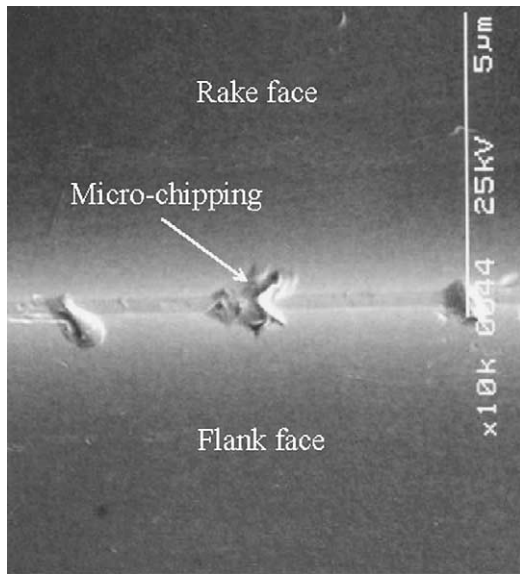
The tools were observed intermittently with an SEM at intervals of every three facing cuts. Three facing cuts give rise to a total cutting distance of 1.27 km. In order to observe and measure the machined surfaces, a Nomarski differential interference microscope, an SEM and a surface-profiling instrument, Form Talysurf, were used, respectively. The cutting chips were also observed using an SEM.

3. Results

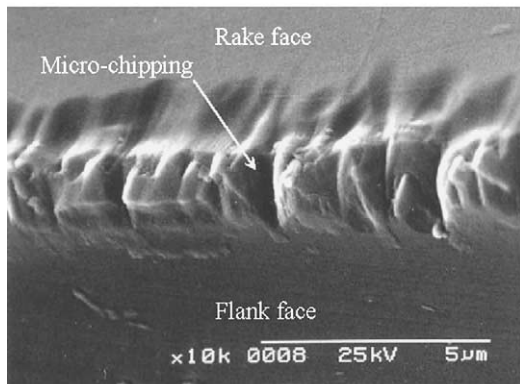
3.1. Tool wear patterns

In the fabrication of curved surfaces such as aspheric optical elements, brittle mode cutting is sometimes needed before performing finish cut in order to achieve a high material removal rate. In this study, first, brittle mode cutting was performed at an undeformed chip thickness of 900 nm under dry conditions. Fig. 4(a) is an SEM photograph of the cutting edge after cutting for 1.27 km. In the figure no obvious wear can be observed on the rake face whereas an extremely small wear land and a few micro-chippings has occurred to the edge. The size of these micro-chippings is approximately $1 \mu\text{m}$, approaching the same level as the undeformed chip thickness. As cutting distance increased, both the number and the size of the micro-chippings increased. Fig. 4(b) is a SEM photograph of the same cutting edge after cutting for 7.62 km. The entire edge has been covered with micro-chippings which are a few micrometers in size.

Next, ductile mode cutting was performed at an undeformed chip thickness of 90 nm. Fig. 5(a) is an SEM photograph of the cutting edge after cutting for 1.27 km. A crater wear has been formed on the rake face, the point of greatest crater depth occurring near the midpoint of contact length. Immediately near the crater wear, a $1 \mu\text{m}$ wide flank wear land is formed. Both the crater wear and the wear land are smooth and uniform along the entire cutting edge, indicating that the tool wear has been a stable and gradual process. As cutting distance increased, the width of the crater did not change significantly whereas the width of the flank wear land kept increasing rapidly. Also, the wear land surface



(a)



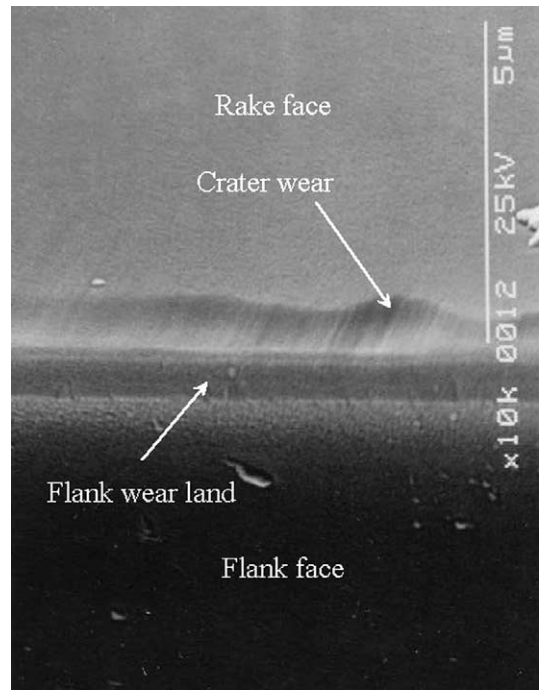
(b)

Fig. 4. SEM photographs of the cutting edge after brittle mode cutting for (a) 1.27 and (b) 7.62 km, respectively, showing occurrence of micro-chippings.

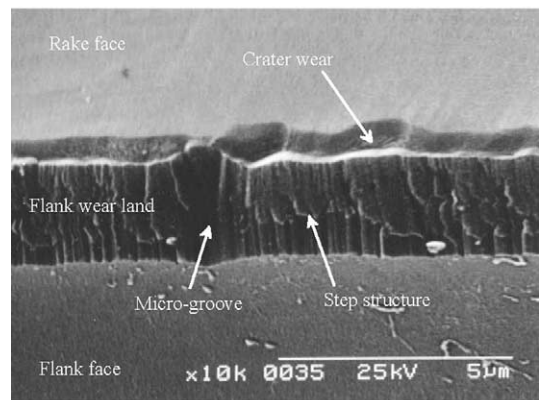
becomes roughened from a cutting distance of 3.81 km. Fig. 5(b) is an SEM photograph of the cutting edge after cutting for 7.62 km. The crater wear on the rake face shows no obvious increase compared with that in Fig. 5(a), but the flank wear land has increased up to 2 mm wide. Unlike that in Fig. 5(a), the flank wear land in Fig. 5(b) is covered with numerous micro grooves oriented along the cutting direction and a step structure can be observed on the wear land. These features indicate that the tool wear has been accelerated and has changed from a steady process to an unsteady process.

3.2. Effects of tool wear on cutting behaviour

Next, the variation in cutting behaviour with tool wear at an undeformed chip thickness of 90 nm was examined. Fig. 6 shows the variation of surface roughness R_y (peak–valley) with cutting distance. The measurement of surface roughness was performed on the $\langle 11\bar{2} \rangle$ orientation of the workpiece,



(a)



(b)

Fig. 5. SEM photographs of the cutting edge after ductile mode cutting for (a) 1.27 and (b) 7.62 km, respectively, showing the changes of crater wear and flank wear land.

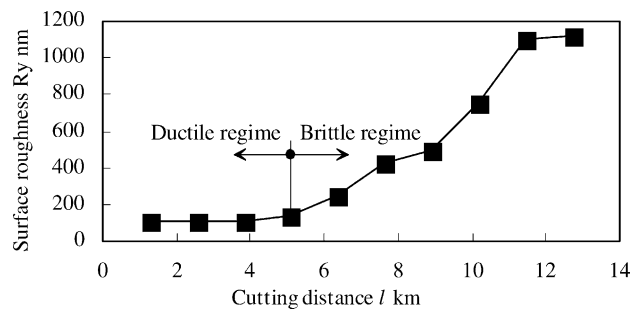
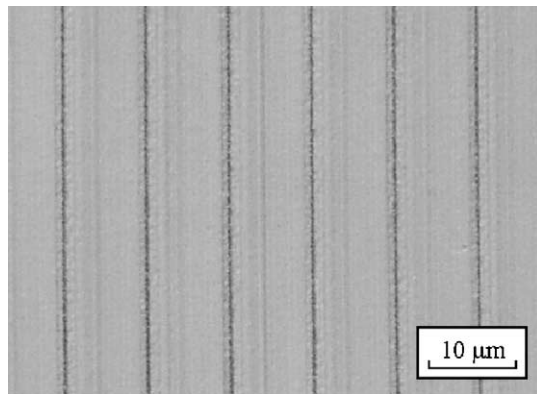
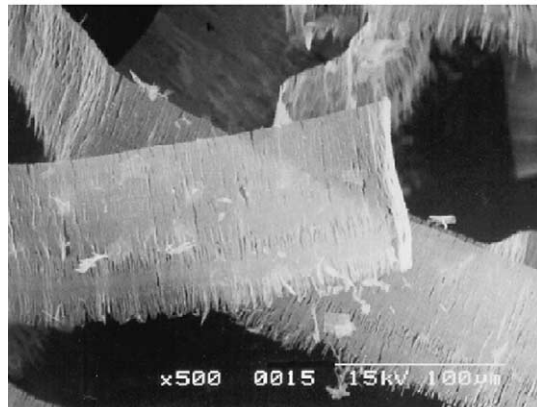


Fig. 6. Variation of surface roughness with cutting distance, indicating the ductile–brittle transition of cutting mode at a cutting distance of approximately 5 km.



(a)

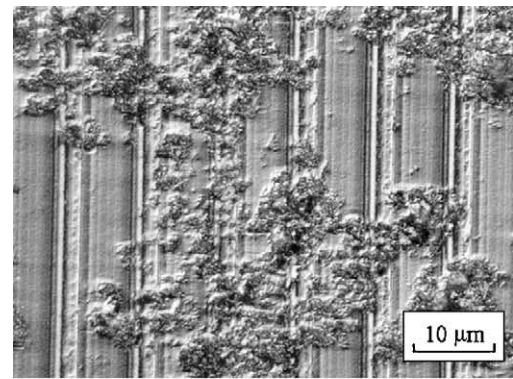


(b)

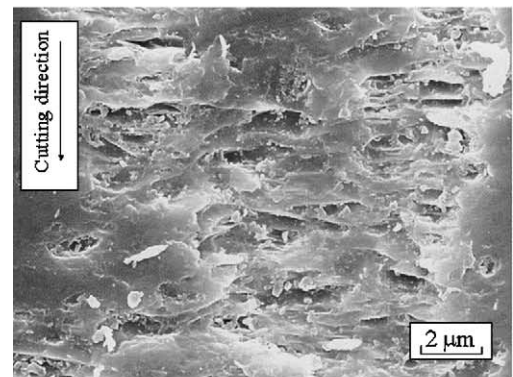
Fig. 7. (a) Nomarski micrograph of the machined surface and (b) SEM photograph of the cutting chips after cutting for 1.27 km at an undeformed chip thickness of 90 nm.

which is the orientation most difficult to be ductile machined. It can be seen that until a cutting distance of 3.81 km, the surface roughness kept almost constant at a low level. However, after 5.08 km the surface roughness began to increase rapidly. The rapid increase in surface roughness indicates the transition of cutting mode from ductile to brittle. Fig. 7(a) is a Nomarski photograph of the machined surface after cutting for 1.27 km. The surface is very smooth with no apparent fractures. Fig. 7(b) is an SEM photograph of the cutting chips formed under the same conditions. These chips are long and continuous ribbon chips, like those of metal cutting. This kind of chip demonstrates a ductile material removal mode.

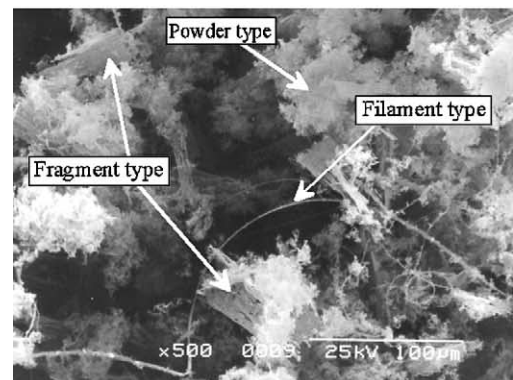
Fig. 8(a) is a Nomarski photograph of the machined surface after cutting for 11.4 km. Although a part of the surface remains smooth, most of the surface has been damaged by adjacent micro-fractures. Fig. 8(b) is a higher magnification SEM photograph of the micro-fractures. The micro-fractures consist of numerous micrometer level cracks oriented perpendicularly to the cutting direction. These micro-fractures are thought to be resulting from the rubbing force generated by the flank wear land of the tool. Fig. 8(c) is an SEM photograph of the chips formed under the same conditions. These chips are discontinuous and can be classified into powder



(a)



(b)

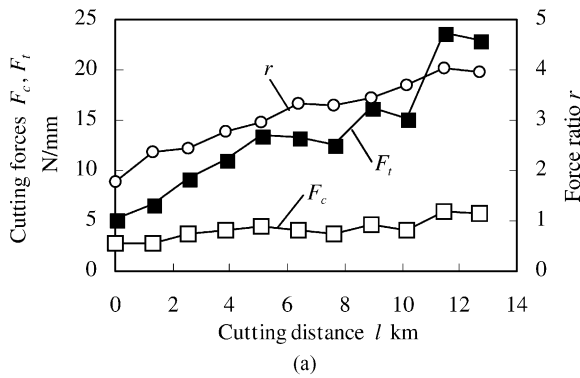


(c)

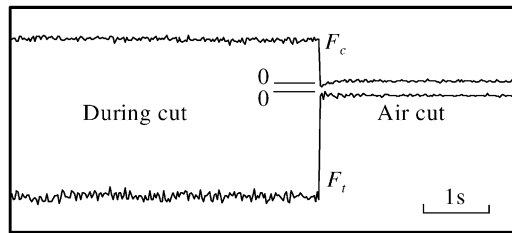
Fig. 8. (a) Nomarski micrograph of the machined surface, SEM photographs of (b) the micro-fractures on the machined surface and (c) the chips after cutting for 11.4 km at an undeformed chip thickness of 90 nm.

type, fragment type and filament type, indicating the unsteadiness of the cutting process.

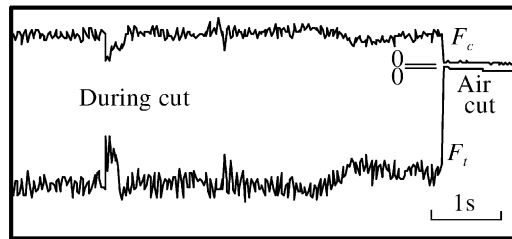
Fig. 9(a) shows the variations in principal force F_c , thrust force F_t per unit of cutting length (mm) and their ratio r with cutting distance. Until the cutting distance of 5.08 km, both F_c and F_t tended to increase linearly. After that, the forces increased with significant fluctuations. Fig. 9(b) and (c) show the force waviness at 1.27 and 7.62 km, respectively. In Fig. 9(b) the force waviness is very steady, whereas in Fig. 9(c) sudden fluctuations can be observed frequently, indicating the unsteadiness of the



(a)



(b)



(c)

Fig. 9. (a) Variations in cutting forces and force ratio; changes in force waviness with cutting distance from (b) 1.27 to (c) 7.62 km at an undeformed chip thickness of 90 nm.

cutting process. From Fig. 9(a), it can also be seen that the force ratio keeps increasing linearly as the tool wears. These results demonstrated the possibility of monitoring the tool wear using cutting force signals.

3.3. Effects of coolant on tool wear

Kerosene mist and water were used as coolants and the results were compared with those of dry cutting. First, the critical chip thickness d_c of silicon under these conditions was measured. The value of d_c was calculated from the critical tool feed (f_c) at the brittle–ductile transition boundary [6], according to Eq. (1). Fig. 10 shows a comparison of critical chip thickness under the dry conditions and the wet conditions. It can be seen that the use of either coolant causes a decrease in critical chip thickness, i.e. leading to lower ductile machinability than dry cutting. However, it was also shown that the use of either coolant has prolonged the ductile mode cutting distance. Fig. 11 shows the changes of surface roughness with cutting distance at an undeformed chip thickness of 60 nm under different coolant conditions.

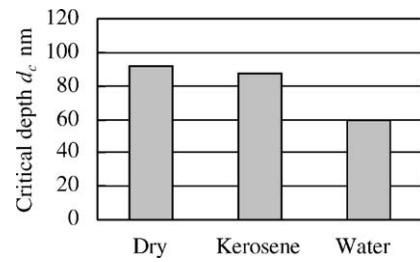


Fig. 10. Variation of critical chip thickness (critical depth, d_c) with coolant conditions.

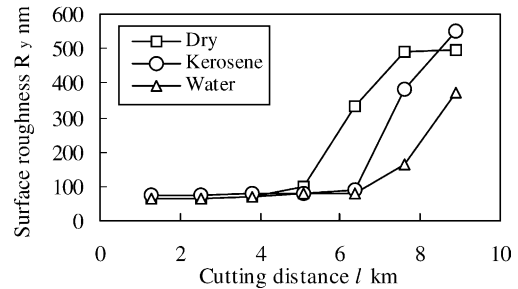


Fig. 11. Variation of surface roughness with cutting distance at an undeformed chip thickness of 60 nm under different coolant conditions, showing that the use of coolants prolongs ductile mode cutting distance.

Compared to dry cutting, the use of water and kerosene mist as coolants resulted in longer ductile mode cutting distances.

4. Discussion

The wear of diamond tools in ultra-precision machining has been the subject of controversial studies and is still not well understood. Several different mechanisms such as mechanical, thermal, chemical and possible electrical effects can contribute to diamond wear and multiple mechanisms may be at work under some circumstances. However, the predominant wear mechanism will depend on machining conditions.

When cutting silicon at the micrometer level, i.e. in brittle mode cutting, cleavage fracturing occurs to the work material, forming micro craters in front of the cutting edge [18]. The micro craters make the cutting process intermittent and cause micro impacts. These micro impacts will take place at a very high frequency, leading to edge chippings. This mechanism may be similar to the fracture of other brittle-material tools in traditional interrupted cutting or when cutting materials containing hard particles and inclusions [11,12,19].

When cutting silicon at an undeformed chip thickness of a few tens of nanometres, i.e. in ductile mode cutting, the initial tool wear tends to be a gradual process and can be considered as the presence of a combination of adhesive wear, abrasive wear and possible diffusion wear. That is, when a diamond tool is new and sharp, conditions on the

rake face are much more severe than those on the flank face. Temperature and pressure are very high and the rake face constitutes a heavily loaded slider [20]. Under such conditions, diffusion wear will be predominant and the characteristic wear pattern is a crater. As cutting distance increases, the cutting edge recedes and the flank wear land becomes predominant. The wear land results in a loss of relief angle, which gives rise to increased friction resistance (cutting forces). The wear land is normally a loaded slider with maximum temperature at the trailing edge which increases with increase in wear land length [20]. The wear rate rises abruptly when the temperature at the trailing edge of the wear land reaches the thermal deterioration point of diamond. The thermal deterioration under these circumstances may involve the diamond–graphite transformation at high temperature [21] and the chemical reaction between carbon, silicon and oxygen. Subsequently the deteriorated layer at the trailing edge drops off due to the rubbing force between the tool and the workpiece, forming step structures on the wear land. This kind of wear is catastrophic and will lead to the total destruction of the tool. The flank wear land also causes unacceptable figure error in the part and induces surface micro-fractures.

While the groove formation on the wear land is a complex problem, whose mechanism is not yet clarified. It is assumed that when the crater wear approaches the cutting edge, micro-chippings occur to the edge and the work material that is not removed by the chipped cutting edge rubs without clearance on the tool, generating micro grooves. Particles of brittle chips left behind on the previously cut surface can also act as small cutting edges to induce wear grooves. The presence of grooves on the cutting edge is a source of surface roughness of the machined surface and dictates tool life in finish machining.

5. Conclusions

Single-crystal silicon has been machined with single point diamond tools and the tool wear characteristics were experimentally investigated. The results can be summarized as given further.

1. Tool wear can be classified into two types: micro-chippings and gradual wear, the predominant wear mechanism depending on undeformed chip thickness. Brittle mode cutting at an undeformed chip thickness of the micrometer level leads to edge micro-chippings; whereas ductile mode cutting at an undeformed chip thickness of a few tens of nanometres causes gradual wear involving crater wear and flank wear land. The flank wear land is initially a smooth surface but eventually becomes roughened by micro grooves and step structures, leading to a total tool failure for ductile mode cutting.
2. Tool wear significantly influences the resulting surface roughness, chip formation and micro-cutting forces. When cutting distance exceeds a critical value (approximately 5 km under the present conditions), the cutting mode transits from ductile to brittle, leaving micro-fractures on the machined surface. The chip changes from a continuous ribbon type to a mixture type of powders, fragments and filaments. The ductile cutting performance of a diamond tool is possible to be monitored using cutting force signals.
3. A coolant has double-face effects on ductile mode cutting. Compared to dry cutting, the use of a coolant decreases the critical chip thickness but prolongs the critical cutting distance for ductile mode cutting.

The future direction of this work involves investigating the chemical and thermal aspects of tool wear mechanism and the effect of diamond crystal orientation on anti-wear performance.

Acknowledgements

This research has been conducted as a part of the project “Fabrication of large aspheric optical elements on single-crystal silicon by ductile regime machining” supported by the Ministry of Education, Science, Sports and Culture, Grant-in-Aid for Encouragement of Young Scientists (Project Number 13750090). A part of this work has also been supported by the grant from the Japan New Energy and Industrial Technology Development Organization (NEDO) (Project Number 01A38004).

References

- [1] T. Nakasuji, S. Kodera, S. Hara, H. Matsunaga, N. Ikawa, S. Shimada, Diamond turning of brittle materials for optical components, *Ann. CIRP* 39 (1) (1990) 89–92.
- [2] P.N. Blake, R.O. Scattergood, Ductile regime machining of germanium and silicon, *J. Am. Ceram. Soc.* 73 (4) (1990) 949–957.
- [3] T. Shibata, S. Fujii, E. Makino, M. Ikeda, Ductile-regime turning mechanism of single-crystal silicon, *Prec. Eng.* 18 (2/3) (1996) 130–137.
- [4] T.P. Leung, W.B. Lee, X.M. Lu, Diamond turning of silicon substrates in ductile-regime, *J. Mater. Process. Technol.* 73 (1998) 42–48.
- [5] J. Yan, M. Yoshino, T. Kuriyagawa, T. Shirakashi, K. Syoji, R. Komanduri, On the ductile machining of silicon for micro electro-mechanical systems (MEMS), opto-electronic and optical applications, *Mater. Sci. Eng. A* 297 (1/2) (2001) 230–234.
- [6] J. Yan, K. Syoji, T. Kuriyagawa, H. Suzuki, Ductile regime turning at large tool feed, *J. Mater. Process. Technol.* 121 (2002) 363–372.
- [7] J. Yan, K. Syoji, T. Kuriyagawa, Fabrication of large-diameter single-crystal silicon aspheric lens by straight-line enveloping diamond-turning method, *J. Jpn. Soc. Precis. Eng.* 68 (4) (2002) 1561–1565 (in Japanese).
- [8] H. Hamada, Diamond tools for ultra-precision machining, *J. Jpn. Soc. Precis. Eng.* 51 (9) (1985) 9–13.
- [9] C.K. Syn, D.A. Krulwich, P.J. Davis, M.R. McClellan, P.C. DuPuy, M.A. Wall, K.L. Blaedel, An empirical survey on the influence of machining parameters in diamond turning of large single crystal silicon optics, in: *Proceedings of the ASPE Spring Topical Meeting on Silicon Machining*, (Carmel-by-the-Sea) California, April 1998, p. 44.

- [10] D. Keen, Some observations on the wear of diamond tools used in piston machining, *Wear* 17 (1971) 195–208.
- [11] R. Wada, H. Kodama, K. Nakamura, Y. Mizutani, Y. Shimura, N. Takenaka, Wear characteristics of single crystal diamond tool, *Ann. CIRP* 29 (1) (1980) 47–52.
- [12] C.J. Wong, Fracture and wear of diamond cutting tools, *transactions of the ASME, J. Eng. Mater. Tech.* 103 (1981) 341–345.
- [13] R.E. Glardon, I. Finnie, Some observations on the wear of single point diamond tools used for machining glass, *J. Mater. Sci.* 16 (1981) 1776–1784.
- [14] J.M. Oomen, J. Eisses, Wear of monocrystalline diamond tools during ultraprecision machining of nonferrous metals, *Prec. Eng.* 14 (4) (1992) 206–218.
- [15] E. Paul, C.J. Evans, A. Mangamelli, M.L. McGlaufflin, R.S. Polvani, Chemical aspects of tool wear in single point diamond turning, *Prec. Eng.* 18 (1) (1996) 4–19.
- [16] W.S. Blackly, R.O. Scattergood, Ductile-regime machining model for diamond turning of brittle materials, *Prec. Eng.* 13 (2) (1991) 95–103.
- [17] J. Yan, K. Syoji, T. Kuriyagawa, Ductile-brittle transition under large negative rake angles, *J. Jpn. Soc. Precis. Eng.* 66 (7) (2000) 1130–1134 (in Japanese).
- [18] J. Yan, K. Syoji, T. Kuriyagawa, Chip morphology of ultraprecision diamond turning of single crystal silicon, *J. Jpn. Soc. Precis. Eng.* 65 (7) (1999) 1008–1012 (in Japanese).
- [19] N. Ikawa, S. Shimada, Microfracture of diamond as fine tool material, *Ann. CIRP* 31 (1) (1982) 71–74.
- [20] M.C. Shaw, *Metal Cutting Principles*, Clarendon Press, Oxford, 1986, p. 209.
- [21] N. Ikawa, S. Shimada, Diamond tools for ultra-precision cutting, *Trans. JSME* 50 (456) (1985) 1321–1326 (in Japanese).